Neurobiology of Disease

Role of External Pallidal Segment in Primate Parkinsonism: Comparison of the Effects of 1-Methyl-4-Phenyl-1,2,3,6-Tetrahydropyridine-Induced Parkinsonism and Lesions of the External Pallidal Segment

Jesus Soares,[1]* Michele A. Kliem,[1]* Ranjita Betarbet,[1] J. Timothy Greenamyre,[1] Bryan Yamamoto,[2] and Thomas Wichmann[1]

[1]Department of Neurology, Emory University School of Medicine, Atlanta, Georgia 30322, and [2]Department of Pharmacology and Experimental Therapeutics, Boston University School of Medicine, Boston, Massachusetts 02118

These experiments re-examined the notion that reduced activity in the external pallidal segment (GPe) results in the abnormalities of neuronal discharge in the subthalamic nucleus (STN) and the internal pallidal segment (GPi) and in the development of parkinsonian motor signs. Extracellular recording in two rhesus monkeys, which had been rendered parkinsonian by treatment with 1-methyl-4-phenyl-1,2,3,6-tetrahydropyridine (MPTP), revealed that the average neuronal discharge rate decreased in GPe but increased in STN and GPi. After MPTP, neurons in all three nuclei tended to discharge in oscillatory bursts. In addition, GABA release in STN (measured with microdialysis) was reduced, indicative of reduced activity along the GPe-STN pathway. Finally, the concentration of glutamic acid dehydrogenase (GAD; measured with autoimmunoradiography) was increased in GPe and GPi, likely reflecting increased striatal input and increased activity of local axon collaterals, respectively. Surprisingly, GAD protein in STN remained unchanged, indicating that the usual assumption that GAD levels are determined primarily by the overall activity of GABAergic elements may be too simplistic. The results from the MPTP-treated animals were compared with results obtained in a second group of three animals with ibotenic acid lesions of GPe. GPe lesions resulted in increased discharge in STN and GPi, comparable with the changes seen after MPTP but did not induce oscillatory bursting and had no behavioral effects. The results indicate that a mere reduction of GPe activity does not produce parkinsonism. Other changes, such as altered discharge patterns in STN and GPi, may play an important role in the generation of parkinsonism.

Key words: **subthalamic nucleus; globus pallidus; microdialysis; lesion; Parkinson's disease; extracellular recording**

Introduction

The basal ganglia participate in larger circuits that also include cortex and thalamus. The striatum is the principal input structure of the basal ganglia, and the internal segment of the globus pallidus (GPi) and the substantia nigra pars reticulata (SNr) are the major output structures, projecting toward thalamus and brainstem. According to conventional anatomical models, basal ganglia input and output structures are linked via a monosynaptic "direct" pathway and a polysynaptic "indirect" pathway that involves the external pallidal segment (GPe) and the subthalamic nucleus (STN). Except for the excitatory glutamatergic efferents from STN, intrinsic connections and basal ganglia output projections are GABAergic and inhibitory (Albin et al., 1989; Alexander and Crutcher, 1990). Dopamine released from terminals of the nigrostriatal projection is thought to modulate basal ganglia activity by inhibiting activity along the indirect pathway and enhancing activity along the direct pathway (Alexander et al., 1990). Given the polarity of connections along direct and indirect pathways, striatal release of dopamine may result in an overall reduction of basal ganglia output.

The same model has been applied to explain aspects of the pathophysiology of parkinsonism. Loss of striatal dopamine is believed to result in increased striatal inhibition of GPe, leading to disinhibition of STN neurons and to increased basal ganglia output from GPi and SNr (Wichmann and DeLong, 2003b). Increased and altered basal ganglia output to the thalamus is thought to disturb cortical processing, which is ultimately responsible for the development of many of the parkinsonian motor signs.

Although generally supported by previous recording and lesioning studies, some of the more recent anatomical and biochemical studies have provided findings that are difficult to reconcile with this model. In particular, these reports have cast doubt on the notion that discharge abnormalities in STN and GPi

Received March 8, 2004; revised May 26, 2004; accepted May 31, 2004.

This work was supported by a grant from the National Institute of Neurological Disorders and Stroke (P01 NS38399; project 4). We give special thanks to Dr. Yoland Smith for helping with the histological work on the animals with pallidal lesions and to Dr. Mahlon DeLong for critical discussions of this study.

*J.S. and M.A.K. contributed equally to this work.

Correspondence should be addressed to Dr. Thomas Wichmann, Department of Neurology, Emory University School of Medicine, Suite 6000, Woodruff Memorial Research Building, 101 Woodruff Circle, Atlanta, GA 30322. E-mail: twichma@emory.edu.

DOI:10.1523/JNEUROSCI.0836-04.2004

 0270-6474/04/246417-10$15.00/0

and parkinsonian motor abnormalities are attributable to reduced GPe activity. Thus, comparisons between 1-methyl-4-phenyl-1,2,3,6-tetrahydropyridine (MPTP)-intoxicated monkeys or parkinsonian patients and their respective controls failed to reveal a significant parkinsonism-related decrease in the number of GPe output neurons expressing the mRNA coding for the GABA-synthesizing enzyme glutamic acid decarboxylase (GAD) (Herrero et al., 1993, 1996a,c), a marker presumed to reflect the electrical activity of GABAergic neurons. Furthermore, the expression of mRNA coding for cytochrome oxidase subunit I was significantly increased in parkinsonian monkeys in neurons of STN, GPi, and SNr, confirming that their activity increased after nigrostriatal denervation, but there was no statistically significant change in GPe (Vila et al., 1997).

The aim of this study was to re-examine whether the GPe-STN projection is underactive in parkinsonism, and whether reduction of neuronal activity in GPe leads to parkinsonian motor signs and electrophysiological abnormalities in STN and GPi similar to those found in parkinsonism (for related experiments in rodents, see Hassani et al., 1996). We measured MPTP-induced changes in neuronal activity and GAD expression in GPe, STN, and GPi, as well as GABA release in the STN. These data were compared with data obtained in monkeys with GPe lesions.

Materials and Methods

General methods

Five animals were used for these studies. All animals underwent initial electrophysiological recording of the activity of STN, GPi, and GPe. In this phase of the experiments, the animals' behavior was also quantified using a battery of behavioral assessment methods.

Two of the animals (monkeys H and I) received intracarotid injections of MPTP to induce hemiparkinsonism. Before and after MPTP treatment, GABA levels in the STN were measured with microdialysis methods as an indication of GABA release from terminals of the GPe-STN projection. In addition, post-MPTP recording studies were performed.

The remaining three animals (monkeys F, K, and X) received lesions of GPe followed by additional recording and behavioral observations. At the termination of the experiments, histological studies were performed in all five animals to verify the targets of electrode penetrations and to delineate the extent of dopaminergic and pallidal lesions.

Animals

The five rhesus monkeys (Macaca mulatta; 4–5 kg) used for these studies were housed under conditions of protected contact housing with *ad libitum* access to standard primate chow and water. Before any of the other procedures, the animals were trained to sit in a primate chair, to adapt to the laboratory, and to permit handling by the experimenter. During injection, recording, and microdialysis experiments, the animals were awake. All experimental protocols were performed in accordance with the National Institutes of Health *Guide for the Care and Use of Laboratory Animals* and the United States Public Health Service Policy on Humane Care and Use of Laboratory Animals (amended 2002). All experiments were approved by the Institutional Animal Care and Use Committee of the Emory University Institutional Biosafety Committee.

Surgical procedure

After completion of behavioral training, metal chambers for chronic recording (inner diameter, 16 mm) were stereotactically positioned over a trephine hole under aseptic conditions and isoflurane anesthesia (1–3%). A chamber directed at the pallidum was placed at an angle of 50° from the vertical in the coronal plane [anterior (A), 12; lateral (L), 10; dorsal (D), 5 Horsley–Clark plane (HcO)], and a chamber aimed at the STN was placed at an angle of 36° from the vertical in the sagittal plane (A, 10; L, 6; D, 2 HcO). The chambers were affixed to the skull with dental acrylic. Metal head holders were also embedded into the acrylic cap to permit head stabilization during the recording and microdialysis procedures.

Electrophysiology experiments

The neuronal activity in GPe, GPi, and STN was recorded extracellularly with tungsten microelectrodes (impedance, 0.5–1.0 MΩ at 1 kHz; Frederick Haer, Bowdoinham, ME). A microdrive (MO-95B; Narishige, Tokyo, Japan) was used to lower the microelectrodes through the dura into the brain, using a 20 gauge guide tube. The electrical signal was amplified (DAM-80 amplifier; World Precision Instruments, Sarasota, FL), filtered (400–10,000 Hz; Krohn-Hite, Brockton, MA), displayed on a digital oscilloscope (DL1540; Yokogawa, Tokyo, Japan), and made audible via an audio amplifier. A tape record of the signal was kept using a video recording adapter (model 3000A; Vetter, Rebersburg, PA). Neurons in the basal ganglia were easily identified by such characteristics as a high-frequency discharge with pauses in GPe, tonic high-frequency discharge in GPi, and a tonic and regular activity in an area of high background activity in the STN.

Because none of the GPe lesions was complete, the possibility exists that the lesion effects may have been specific for a particular topographic region within the GPe (for instance, the motor or associative territories). To detect the effects of GPe inactivation, it would thus be desirable to restrict recording to functionally related areas of GPi and STN. With the lateral coronal approach to the globus pallidus chosen for this study, functionally related regions of GPe and GPi are (approximately) aligned along a given electrode track. Thus, by restricting GPi recordings to those cells that followed an electrophysiologically silent (lesioned) portion of GPe, we restricted recording in GPi to cells that are (presumably) functionally related to the lesioned portion of GPe. It was not possible to restrict the analysis in a similar manner in the STN.

Microdialysis

Probe assembly and calibration. Dialysis probes were made with a dual silica tube, parallel flow design (Olson and Justice, 1993). The shaft of the probes was 15 cm long and was made of 27 gauge stainless-steel tubing (Small Parts, Miami, FL). The inflow and outflow tubes were inserted into the 27 gauge stainless-steel tubing and consisted of two pieces of fused silica [inner diameter (i.d.), 0.04 mm; outer diameter (o.d.), 0.1 mm; Polymicro Technologies, Phoenix, AZ]. The inflow tube extended beyond the distal end of the outflow tube by the length of the active dialysis area of the membrane. A short piece of hollow dialysis membrane tubing (i.d., 0.2 mm; cutoff molecular weight, 13,000; Polymicro Technologies) was placed over the ends of the inflow and outflow silica tubes. Epoxy glue (two-ton clear epoxy; Devcon, Chicago, IL) was used to seal the open end of the microdialysis membrane and the junctions between the microdialysis membrane and the inflow and outflow silica tubes. The assembled dialysis membrane and the inflow and outflow silica tubes were glued to the 27 gauge stainless-steel tubing with white epoxy (Devcon). The exposed surface of the hollow dialysis membrane tubing of the probe was 2 mm. The inflow line of the microdialysis system was connected to Teflon tubing (o.d., 0.65 mm; i.d., 0.12 mm; Bioanalytical Systems, West Lafayette, IN) via a liquid switch syringe selector (CMA Microdialysis, Solna, Sweden) to a 1 ml syringe (Bioanalytical Systems) and perfused with artificial CSF (aCSF; in mM: 145 NaCl, 2.8 KCl, 1.2 $MgCl_2$, 1.2 $CaCl_2$, pH 7.2–7.4) at a flow rate of 2 μl/min with a microdialysis syringe pump (Bioanalytical Systems). For a 20 min period in each experiment (see below), the system was perfused with aCSF containing 80 mM K^+. In these experiments, the concentration of NaCl was lowered to maintain osmolality (in mM: 67.8 NaCl, 80 KCl, 1.2 $MgCl_2$, and 1.2 $CaCl_2$).

The dead volume of connecting tubes and the probes themselves were calculated to synchronize microdialysate collection with the timing of switches to aCSF exposure. The *in vitro* relative recovery was calculated by determining the ratio of GABA peak height measured in an equivalent volume of aCSF containing a known amount of GABA. The recovery of the probes ranged from 15 to 20% at flow rate of 2 μl/min by using the aCSF solution.

Microdialysis protocol. Before use, the probes were placed into aCSF and were thoroughly flushed with aCSF at a rate of 2 μl/min for 20 min.

The probes were then slowly inserted into the STN using the microdrive and guide cannula described above. The exact target coordinates were determined by the results of the previous electrophysiological recording experiments. Before sample collections, the probes were perfused with normal aCSF for 2 hr to allow stabilization of the basal GABA concentration before the start of sample collection. Pilot experiments with the techniques used here have shown that the measured GABA levels stabilized 90–120 min after insertion of the microdialysis probes into the brain. In each experiment, eight dialysis samples were collected (20 min; 40 μl/sample) in plastic microcentrifuge tubes. The first five samples were collected without additional intervention, but the perfusion media was changed for the duration of sample 6 to one containing 80 mM K^+ (see above) using a liquid switch syringe selector (CMA Microdialysis). The potassium stimulation of the tissue was used primarily to assess the neuronal origin of GABA.

For the last two samples of the protocol, the probe was again perfused with standard aCSF solution. All samples were immediately placed on dry ice and later stored at −80°C until the time of analysis. At the termination of each microdialysis session, the probe was removed, the chamber was cleaned, and the animal was put back in its home cage. The same animal underwent multiple microdialysis procedures, separated by at least 24 hr. For each microdialysis session, a new track was used to sample undisturbed tissue.

Administration of MPTP

After completion of recording and microdialysis procedures in the normal state, monkeys H and I received MPTP by injection into the right carotid artery (0.5 mg/kg per injection; monkey H received two injections 36 d apart; monkey I received one injection), following reported standard protocols (Bankiewicz et al., 1986). Both animals showed clear parkinsonian signs on the side contralateral to the injections (i.e., on the left side of their body) after these injections, including bradykinesia, rigidity, and flexed limb posture. The post-MPTP experiments started 2 months after the last MPTP injection.

GPe lesioning procedure

These studies were performed in monkeys F, K, and X. The animals received multiple small (0.2–0.5 μl, 0.2 μl/min) injections of the fiber-sparing excitotoxin ibotenic acid (10 mg/ml, dissolved in bidistilled water on ice, final pH 7.4; Sigma, St. Louis, MO) into GPe. The injections were performed with a combined injection-recording device, which permits electrophysiological recording before and during injections to verify injection location. The device consists of a 30 gauge injection cannula through which a Teflon-coated tungsten recording wire (0.05 mm bare diameter, 0.076 mm coated diameter; AM Systems, Carlsborg, WV) was threaded, the tip of which protrudes 0.2–0.7 mm from the cannula. The device was passed through the dura through a guide tube. Gray and white matter areas of the brain were easily identified with this system, facilitating the identification of injection targets. The injections were delivered over several days. The volume of the individual injections was kept to a minimum to limit the spread of the toxin. Between drug injections, the amount of damage produced by the toxin was assessed by additional electrophysiological mapping. The series of injections was terminated once the accessible GPe was electrophysiologically silent. Monkey F received a total of 115 μg of ibotenic acid, whereas monkey K received 33 μg and monkey X received 29 μg.

Behavioral assessment method

Behavioral changes associated with GPe inactivation, as well as parkinsonian signs associated with MPTP treatment, were documented through observations of spontaneous cage behavior. For quantification, one of the investigators (J.S. for the MPTP-treated animals; M.K. for the GPe lesioned animals) used a computer-assisted behavioral scoring system to score the occurrence of spontaneous limb movements in an observation cage over a 20 min period. The system has been used previously and has been validated in the context of other studies (Bergman et al., 1990; Wichmann et al., 2001a). Briefly, each time the animal moved one of its extremities, a computer keyboard key assigned to this extremity was pressed and held down for the duration of the movement. The ratio of arm movements registered on the left side and those registered on the right side was used as an index of arm movements.

We also used an automated activity monitoring system. The observation cage was equipped with eight infrared beams. Four of these beams were arranged in a square design between the back and the front of the cage, and four additional beams, arranged in a similar manner, between the two sides of the cage. An attached computer kept a log of the timing of infrared beam crossings. Off-line, the system then calculated total activity counts. The 20 min activity monitoring periods were also videotaped.

All observations were performed at the same time of day. The behavioral assessment method was used before and twice weekly after completion of the MPTP treatment and of GPe lesions.

Histology

At the conclusion of the experiments, the monkeys were killed by induction of deep anesthesia with an overdose of sodium pentobarbital, followed by transcardial perfusion with saline and 4% paraformaldehyde in 0.1 M phosphate buffer (PB), pH 7.2. The brains were removed and cryoprotected in a 30% sucrose solution in 0.1 M PB. The fixed brain was sectioned in coronal planes (50 μm). One of every four sections was stained with cresyl violet. In the case of the MPTP-treated animals, the remaining sections were used for double-labeling studies to visualize GAD and tyrosine hydroxylase (TH). In the GPe-lesioned animals, sections were used to label the neuronal marker microtubule-associated protein 2 (MAP2) using standard immunohistochemistry protocols.

For the double-labeling studies, sections were thoroughly washed in 0.1 M Tris-buffered saline (TBS), to remove the cryoprotectant and incubated in 10% normal goat serum with 0.04% Triton X-100 in TBS for 30 min. Thereafter, they were incubated for 72 hr in the same solution containing either a primary antiserum or a mixture of primary antibodies. The antibodies used for this study were against TH (1:1000, mouse monoclonal antibody; Chemicon, Temecula, CA) and GAD (1:2000, rabbit polyclonal antibody; Chemicon). Next, the sections were rinsed in 0.1 M TBS and incubated for 2 hr with goat anti-rabbit antibody conjugated to ^{125}I (for GAD) and biotinylated goat anti-mouse antibody (for TH). For enzyme-linked staining of TH-positive cells or GAD, the biotin–avidin complex method was used, whereas 3,3′-diaminobenzidine tetrachloride was used to visualize the final product. For control sections, either one or both of the primary antibodies were omitted. Finally, the sections were rinsed in 0.1 M TBS, mounted on gelatin-coated slides, and air-dried. The slides were placed in x-ray cassettes with calibrated ^{125}I standards (Amersham Biosciences, Piscataway, NJ) and apposed to Hyperfilm3H (Amersham Biosciences) for 2–3 weeks. The films were developed in D-19, fixed in Kodak (Rochester, NY) fixer, and dried.

Data analysis

Analysis of behavioral data. To analyze the detailed cage observation records, a ratio of the durations was computed (within the 20 min observation period), during which the left and the right arm, or the left and right leg, were used. These left/right (L/R) ratios were used as indicators of parkinsonian hypokinesia (Bergman et al., 1990). The L/R ratios and activity monitoring scores were then plotted over time, comparing the post-MPTP or postlesion data with data obtained in the normal state. Because there were no obvious changes over time in the L/R ratios or activity counts after the MPTP or GPe lesions, the postintervention data were pooled for each monkey and compared with the preintervention data for the respective animal.

Analysis of electrophysiological data. Only those cells in which reconstruction of their location, on the basis of stereotactic information, location, and depth data gathered during the actual recordings as well as histological analysis of the cresyl violet stained sections, confirmed that they were within the target structures (GPe, GPi, or STN) were included in the analysis. To generate interspike interval (ISI) information, the tape-recorded activity was passed through a template-matching spike sorter (Alpha-Omega, Nazareth, Israel). The subsequent analysis used the Matlab software environment (MathWorks, Natick, MA). Neuronal data were included in this study only if the isolation of the respective cell could be maintained throughout the record, if at least 1000 action poten-

tials had been recorded, and if the spontaneous activity of the neuron was recorded for at least 45 sec. Most neurons were, in fact, recorded far longer (mean, 339.5 sec). The ISI data were converted into frequencies, and a power spectral analysis of the frequency representation (sampled at 100 Hz) was performed, using Hanning windows and mean detrending of data segments. For statistical analysis, the elements of the ISI data stream were randomly shuffled, and the power spectrum of the resulting (random) data stream was calculated. Both power spectra were smoothed with a 10 point moving average. The mean and SD of the resulting power spectrum of the shuffled data were computed. Peaks in the power spectra of the original data stream were considered significant only if 10 consecutive points of the spectrum were at least 5 SD different from the mean of the shuffled data.

Bursts were detected using an algorithm developed by Legendy and Salcman (1985). The algorithm is based on the Poisson "surprise" method. For this analysis, a surprise value of 10 was used. For each cell, we calculated a burst index (i.e., the ratio between the number of spikes found in bursts and the total number of spikes).

Chemical analysis. The concentration of GABA in the dialysate samples was determined by HPLC with electrochemical detection as described previously by Donzanti and Yamamoto (1988). Briefly, GABA was assayed by precolumn derivatization with *o*-phthaldialdehyde. The derivatization reagent was prepared by dissolving 27 mg of *o*-phthaldialdehyde in 1 ml of 100% methanol, 9 ml of 0.1 M sodium tetraborate, pH 9.4, and 10 ml of β-mercaptoethanol. This stock solution was then diluted 1:3 with 0.1 M sodium tetraborate. A 10 ml aliquot of the reagent solution was then added to 20 ml of the dialysate sample. Derivatization was allowed to proceed for 30 sec before injection onto a 3 mm C18 reverse-phase column (100 × 2.0 mm; Phenomenex, Torrance, CA) maintained at 32°C. GABA was eluted with a 0.1 M sodium phosphate mobile phase, pH 6.4, containing 23% methanol and 50 mg/l Na_2EDTA. Mobile phase was pumped through the system at a flow rate of 0.3 ml/min. Detection of GABA was at a glassy carbon electrode (6 mm diameter) maintained at +0.7 V by an LC4B amperometric detector (Bioanalytical Systems). The limit of detection for GABA was 8.5 pg/20 ml (3:1 signal-to-noise ratio).

Analysis of microdialysis data. The effect of potassium stimulation was clearly visible in sample 6 (the time of stimulation) and sample 7 (washout period). In each experiment, the basal level of GABA was calculated as the average of samples 1–5 and 8. The stimulation-evoked GABA overflow was calculated by subtracting the basal level (as defined above) from samples 7 and 8 and adding the resultant measurements. For graphical representation (see Fig. 3*A*,*B*), all values were normalized to the average basal level in the normal state.

Analysis of double-labeling studies. Images were collected on a Leitz (Wetzlar, Germany) microscope linked to a microcomputer imaging device (MCID) image analysis system (Imaging Research, St. Catharines, Ontario, Canada). For final output, images were composed using Adobe Photoshop (Adobe Systems, San Jose, CA).

For densitometric measurements of GAD immunoreactivity (GAD-IR), the autoradiograms were analyzed with a video-based MCID image analysis system by relating optical density to calibrated ^{125}I standards. Eight sections from the globus pallidus and six sections from the subthalamic nucleus from each of the monkeys used for the study were analyzed. Data from the untreated side were compared with the data from the lesioned side in unilaterally treated monkeys. GAD-IR was expressed as percentage control.

Analysis of lesion location in the GPe-lesioned animals. Microscopic images of cresyl violet and MAP2-stained sections were collected using a Leitz microscope. The lesion extent, as judged by the absence of MAP2 staining, was first drawn on serial images of the cresyl violet-stained sections. The outlines of the basal ganglia nuclei as well as the lesion locations were then transferred into line drawings (see Fig. 5). The approximate anterior coronal coordinate of the planes shown in Figure 5 was estimated on the basis of atlas information (Winters et al., 1969) and the number of the histological slices within the series of sections.

Statistical analysis. Statistical comparisons were performed in the Statistical Program for the Social Sciences environment. The neuronal data from the different monkeys within the same experimental group or period (normal, MPTP-lesioned, GPe-lesioned) were pooled after exclusion of intersubject differences with ANOVA. Statistical tests for significance were performed with *t* tests (with Bonferroni correction for multiple comparisons). A p level < 0.05 was accepted as indicating a significant difference.

Results

Behavioral observation

Both of the MPTP-treated animals developed marked hemiparkinsonism on the side contralateral to the injections. On the affected (left) side, manipulations of objects was greatly impaired, the animals stopped grooming or feeding themselves with the affected arm, and they held their arm and leg in a flexed position. The whole body posture was also markedly stooped. However, by using the right arm, the animals were able to maintain themselves and, in fact, gained weight in the post-MPTP phase. The global activity of the animals was not markedly impaired, because they developed a prominent tendency to circle toward the hemiparkinsonian side in their cages.

Behavioral assessment with the computer-assisted observation system (Bergman et al., 1990) revealed that spontaneous arm and leg movements became markedly asymmetric because of reduced use of the parkinsonian arm. In monkey I, the L/R ratio for arm movements decreased from a pre-MPTP value of 0.83 ± 0.15 ($n = 4$) to a post-MPTP value of 0.08 ± 0.05 ($n = 16$; $p < 0.01$). In monkey H, only one pre-MPTP assessment was available, showing an L/R ratio of 0.75. After MPTP, the L/R ratios decreased to 0.32 ± 0.06 ($n = 8$). Similar results were obtained for leg movements. Throughout the recording and microdialysis sessions, the behavioral state remained stable in both animals. All of these findings are typical responses to intracarotid MPTP treatments.

In the GPe-lesioned animals, parkinsonism or other motor abnormalities were not detected by direct cage observations, activity monitoring, or the computer-assisted behavioral observation system.

Electrophysiological recordings

Because most of the observed effects were consistent between animals, we will describe these changes here only as averages across monkeys (Figs. 1, 2). The electrophysiological data for individual animals are listed in Table 1.

Discharge rates

MPTP treatment resulted in obvious changes in discharge rates and discharge patterns in GPe, STN, and GPi (Fig. 1, Table 1). In the MPTP-treated state, the average neuronal discharge rate (Fig. 1*A*) in GPe decreased from a control value of 65.1 ± 2.9/sec ($n = 66$ neurons; mean ± SEM) to 45.9 ± 2.6/sec ($n = 53$ neurons; $p < 0.001$; *t* test). In contrast, MPTP treatment induced an increase in the average discharge rate of STN neurons from a control value of 25.7 ± 1.2/sec ($n = 85$) to 36.1 ± 1.6/sec ($n = 45$; $p < 0.005$), and in GPi from 65.1 ± 1.8/sec ($n = 134$) to 80.6 ± 3.1/sec ($n = 40$; $p < 0.001$). There were no discernible regional differences in the distribution of GPe, STN, or GPi cells with high or low discharge rates.

Prominent discharge rate abnormalities were also evident in the GPe-lesioned animals. After the lesion, the average rate of discharge in the STN rose from the above-mentioned control of 25.7 ± 1.2 to 36.0 ± 2.2/sec ($n = 74$; $p < 0.01$). This was significant in both animals for which STN data were available (Table 1). In GPi, the average rate rose from 65.1 ± 1.8 to 69.3 ± 2.0/sec ($n = 137$). The mean rate increased in all three animals, but this reached significance only in one (Table 1) and was not significant in the aggregate. There were no discernible regional differences in the distribution in STN or GPi of cells with high or low discharge

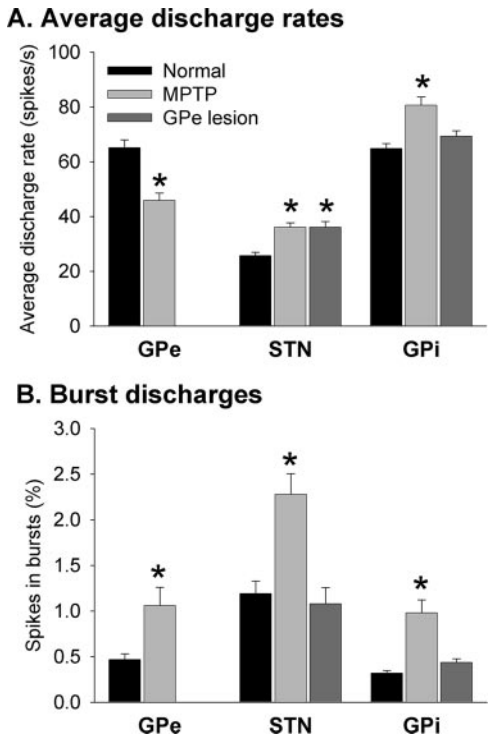

Figure 1. Comparison of changes in neuronal discharge in GPe, STN, and GPi in parkinsonian and GPe-lesioned primates. *A*, Changes in average discharge rates. The black columns show the discharge rates (mean ± SEM) under normal conditions; the light gray columns were derived from data of monkeys H and I after treatment with MPTP, and the dark gray columns were derived from monkeys F, K, and X after placement of GPe lesions. *B*, Changes in the percentage of neuronal discharge detected within bursts. Same conventions as in *A*. *$p < 0.05$ versus data in the normal state. See text for *n* numbers.

rates. However, as mentioned in Materials and Methods, the recording in GPi was restricted to an area functionally related to the lesioned portion of GPe, whereas no effort was made to restrict the recording to any particular territory within STN. GPe lesions and MPTP-induced depletion of striatal dopamine resulted in similar changes in the overall discharge rates in STN and GPi.

Discharge patterns

In addition to the abnormalities in neuronal discharge rate, there were also obvious changes in discharge patterns in the MPTP-treated animals (Figs. 1, 2). The incidence of burst discharge (Fig. 1*B*), subjectively noted during the recording sessions and objectively assessed with the burst-detection algorithm, increased in GPe from 0.47 ± 0.06% in the normal state to 1.1 ± 0.2% in the MPTP-treated state ($p < 0.05$), in STN from 1.28 ± 0.15 to 2.28 ± 0.22% ($p < 0.001$), and in GPi from 0.32 ± 0.03 to 0.98 ± 0.14% ($p < 0.001$).

In contrast, the incidence of burst discharges did not change in the GPe-lesioned animals in STN or GPi, either subjectively or objectively. In STN, the postlesion incidence of bursts was 1.08 ± 0.18% (see above for control values), and in GPi, the postlesion incidence of bursts was 0.44 ± 0.02% (Fig. 1*B*).

Changes in oscillatory discharge were assessed using autocorrelograms and power spectra (as detailed in Materials and Methods). As noted previously, recordings in the MPTP-treated animals revealed that neurons in GPe, STN, and GPi developed a strong tendency to burst in an oscillatory manner in the parkinsonian state. Integration of power spectra in 1–3, 3–8, 8–15, and 15–50 Hz spectral frequency bands revealed that MPTP treatment induced substantial changes in the power spectral content of the neuronal discharge. In all three structures, the 3–8 and 8–15 Hz bands became more prominent (Fig. 2*A*, Table 1). In STN and GPi, the spectral content in the 1–3 Hz range was also enhanced (data not shown). In GPe, the 1–3 Hz frequency range was less strongly represented. In all structures, the spectral content in the 15–50 Hz range was reduced after MPTP treatment (data not shown). Autocorrelation analyses showed substantial increases in the number of cells with peaks in their autocorrelograms indicative of oscillations in the 3–8 and 8–15 Hz ranges (Fig. 2*B*). In contrast, neither the power spectral analysis nor the analysis of autocorrelograms revealed any changes in the incidence of oscillatory discharge in STN or GPi in the GPe-lesioned animals (Fig. 2*A*,*B*). In fact, the postlesion recordings were virtually identical in this regard compared with those obtained before lesioning. These results indicate that GPe-lesioned and MPTP-treated animals differed substantially with regard to the induction of phasic discharge abnormalities.

Microdialysis experiments

These experiments were aimed at elucidating the effects of dopamine depletion and were, therefore, only performed in monkeys H and I before and after treatment with MPTP (Fig. 3). The basal concentration of GABA in microdialysate samples from the STN in the normal state amounted to 93.8 ± 6.9 pg/20 μl in monkey H and 65.5 ± 7.1 pg/20 μl in monkey I. As shown in Figure 3, *A* and *B*, baseline GABA levels were stable throughout the sampling period. Exposure of the tissue to 80 mM K^+ resulted in a substantial increase in GABA efflux. The evoked overflow amounted to 3.4 times the basal level of GABA in monkey H and 3.3 times the basal level of GABA in monkey I. Compared with the normal state, the basal level of GABA was reduced by an average of 45.3% in monkey H and 35.2% in monkey I (Fig. 3*C*). The stimulated overflow was reduced by 52% in monkey H and 47% in monkey I.

Histology

Cresyl violet staining of coronal sections showed gliosis along microelectrode tracts in all of the animals. Although reconstruction of microelectrode tracts aimed at GPe or GPi was straightforward, tracts aimed at the STN were difficult to reconstruct because these tracts were not in the plane of histological sections. All data from penetrations in which placement of the probes were in doubt were excluded from the analysis. In the MPTP-treated animals, immunohistochemistry for TH (Fig. 4*A*, top) showed that there was a massive loss of dopaminergic terminals in the striatum on the side of the MPTP treatment (right). The loss was most pronounced in the dorsal striatum, whereas the dopaminergic supply to the ventral striatum was relatively preserved.

GAD staining in the MPTP-treated animals revealed that the distribution of GAD-IR was uniform throughout the neuropil of both GPi and GPe in control animals. GAD-IR was also observed in the STN. GAD-IR was increased in the GPe and GPi on the lesioned side in the unilaterally MPTP-lesioned monkeys (Fig. 4*B*). The densitometric analysis confirmed an increase in GAD-IR in GPe and GPi (Fig. 4*C*) ($p < 0.05$). In contrast, GAD-IR was not significantly changed in the STN (Fig. 4*C*) on the parkinsonian side.

Cresyl violet and MAP2 staining of coronal sections throughout the basal ganglia revealed that all three of the GPe-lesioned animals had substantial lesions covering portions of GPe (Fig. 5). The recording chamber placement in monkey F precluded lesioning of the entire GPe. In this animal, the lesion covered the dorsal (predominantly nonmotor) territory of GPe. In the other two animals, the lesions were more extensive and included nonmotor and motor territories of the nucleus. In each case, the core

of the lesion (as judged by MAP2 staining) was surrounded by a halo of gliosis, which was readily visible on cresyl violet staining. Despite our attempts to limit the lesion to GPe, some of the neighboring portions of striatum and GPi were involved in these (fiber-sparing) lesions.

Discussion

Our results corroborate the view that GPe activity is reduced in parkinsonism, and that this reduction may account for the changes in discharge rates in STN and GPi in this disorder. However, a mere reduction in GPe activity does not appear to be sufficient for the development of changes in basal ganglia discharge patterns or motor dysfunction in parkinsonism.

Global neuronal activity changes in parkinsonism

The findings of reciprocal discharge rate changes in GPe and GPi, and of increased rates in STN (Miller and DeLong, 1987; Albin et al., 1989; DeLong, 1990; Filion and Tremblay, 1991; Bergman et al., 1994), have given rise to the notion that most parkinsonian abnormalities result from changes in the indirect pathway of the basal ganglia (Albin et al., 1989; DeLong, 1990). Striatal dopamine loss is postulated to result in increased striatal inhibition of GPe, which in turn results in disinhibition of STN and increased basal ganglia output from GPi. This concept is supported by the fact that STN inactivation results in a substantial reduction of the severity of parkinsonian motor signs in monkeys (Bergman et al., 1990; Guridi et al., 1993; Baron et al., 2002) and human patients (Sellal et al., 1992; Gill and Heywood, 1997; Alvarez et al., 2001).

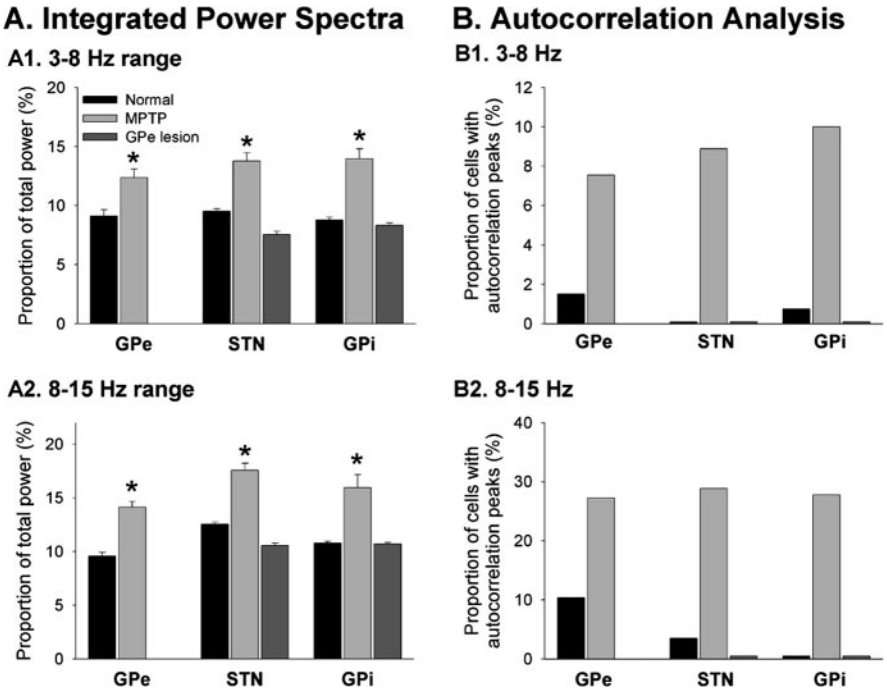

Figure 2. Comparison of oscillatory neuronal activity in GPe, STN, and GPi in parkinsonian and GPe-lesioned animals. *A*, Integrated power spectra. Shown are the ratios of integrated power found in the 3–8 Hz (*A1*) and 8–15 Hz (*A2*) ranges to the total power found in power spectra of neuronal activity, computed between 1 and 50 Hz (see Materials and Methods for computation and Results for additional details). *B*, Autocorrelation analysis. The columns depict the proportion of cells with three or more peaks in the autocorrelograms of their discharge, divided into different frequency ranges (*B1*, 3–8 Hz range; *B2*, 8–15 Hz range). $*p < 0.05$.

Our electrophysiological and microdialysis findings confirm the proposed global activity changes in GPe, STN, and GPi in parkinsonism. We found that the average discharge rate of GPe neurons was significantly decreased. As a further indication of reduced activity of GABAergic GPe cells, the release of GABA in the STN, which is derived in large part from GPe inputs, was reduced by ~50%. Measurements of discharge rates in subsequent stages of the indirect pathway (STN and GPi) confirmed that average discharge in these areas is substantially increased in parkinsonism, which is likely the result of reduced inhibition via GPe efferents (see also below).

The interpretation of the GAD protein measurements is less straightforward. The levels of GAD protein or of GAD mRNA are often used as measures of the activity of GABAergic cells or terminals. This explanation can serve to interpret the finding of increased GAD protein levels in GPe, which may result from increased GABAergic inputs from striatum (Robertson et al., 1991).

GAD protein levels in GPi were also increased in the MPTP-treated animals. In general, GAD levels in GPi may reflect the activity of GABAergic afferents from striatum or GPe or of local axon collaterals. However, it is unlikely that activity changes in the two major GABAergic afferent pathways account for the observed change in GAD activity. As mentioned above, based on electrophysiological and microdialysis findings, the activity of GPe neurons and, thus, of the GPe-GPi projection is reduced in parkinsonism. Based on measurements of striatal GAD mRNA levels, it is also known that striatal neurons projecting to GPi are not overactive in MPTP-treated monkeys (Soghomonian and Laprade, 1997). It is therefore most likely that the increased level of GAD protein in GPi represents increased activity of local axon collaterals of GPi neurons and is therefore another indicator that GPi activity is enhanced in MPTP-treated animals. This is also suggested by studies that have demonstrated that GAD mRNA levels in GPi are increased in parkinsonism (Pedneault and Soghomonian, 1994; Soghomonian et al., 1994; Herrero et al., 1996a; Salin et al., 2002; Schneider and Wade, 2003).

GAD protein levels in the STN would be expected to reflect changes in the activity along the GPe-STN pathway. The finding of unchanged GAD levels in the STN in our study mirrors the results from previous studies, which have shown that GAD65 mRNA remains the same after induction of parkinsonism (Soghomonian and Chesselet, 1992; Pedneault and Soghomonian, 1994; Schneider and Wade, 2003), whereas the level of GAD-67 mRNA in GPe was increased (Soghomonian and Chesselet, 1992; Delfs et al., 1995; Herrero et al., 1996a; Schroeder and Schneider, 2001; Schneider and Wade, 2003). It is obvious that these findings do not agree with the electrophysiological recording and microdialysis data that indicate that GPe activity is substantially decreased. Thus, the assumption that measurements of GAD mRNA or GAD protein levels simply reflect the overall activity of GABAergic neurons may not apply in this case. The regulation of GAD mRNA or protein may be influenced by factors other than discharge rate such as changes in discharge patterns, the emergence of burst discharges, or oscillatory activity. Interestingly, STN lesions abolish the increase in GAD mRNA in GPe in par-

Table 1. Electrophysiological properties of neurons recorded in GPe, STN, and GPi in individual monkeys

Monkey	Nucleus	Condition	Average discharge rate (spikes/sec)	Proportion of spikes in bursts (%)	Spectral content (%)		Proportion (%) of cells with oscillatory autocorrelogram		*n*
					3–8 Hz	8–15 Hz	3–8 Hz	8–15 Hz	
H	GPe	Control	65.3 ± 4.5	0.57 ± 0.09	9.90 ± 0.89	9.89 ± 0.52	2.7	8.1	37
		MPTP	46.6 ± 4.2[a]	1.42 ± 0.41[a]	14.86 ± 1.32[a]	16.78 ± 0.91[a]	13.0	39.1	23
	STN	Control	27.7 ± 2.0	2.08 ± 0.26	10.42 ± 0.36	13.35 ± 0.37	0	11.1	27
		MPTP	35.2 ± 2.3[a]	2.62 ± 0.22[a]	15.72 ± 0.87[a]	19.38 ± 0.75[a]	7.4	33.3	27
	GPi	Control	65.5 ± 4.3	0.57 ± 0.06	11.80 ± 0.59	11.69 ± 0.35	0	0	25
		MPTP	80.4 ± 4.2[a]	1.32 ± 0.23[a]	17.20 ± 1.46[a]	20.83 ± 2.10[a]	16.7	55.6	18
I	GPe	Control	64.8 ± 3.5	0.34 ± 0.06	8.14 ± 0.37	9.18 ± 0.38	0	13.3	29
		MPTP	45.4 ± 3.4[a]	0.79 ± 0.15[a]	10.44 ± 0.56[a]	12.09 ± 0.35[a]	6.7	18.2	30
	STN	Control	24.6 ± 1.9	1.16 ± 0.32	8.70 ± 0.61	11.81 ± 0.43	0	0	11
		MPTP	37.4 ± 2.2[a]	1.77 ± 0.27	10.88 ± 0.65[a]	14.90 ± 0.71[a]	11.1	22.2	18
	GPi	Control	70.3 ± 3.3	0.18 ± 0.02	7.76 ± 0.32	9.85 ± 0.33	0	0	38
		MPTP	80.8 ± 4.6	0.70 ± 0.17[a]	11.33 ± 0.47[a]	11.98 ± 0.49[a]	4.5	5	22
F	GPi	Control	61.9 ± 4.8	0.78 ± 0.17	11.86 ± 1.09	10.57 ± 0.56	0	0	10
		GPe lesion	71.8 ± 2.6[a]	0.75 ± 0.08	10.55 ± 0.34	11.08 ± 0.22	0	0	46
K	STN	Control	24.9 ± 2.5	0.62 ± 0.11	9.22 ± 0.51	12.33 ± 0.42	0	0	16
		GPe lesion	34.2 ± 3.3[a]	0.50 ± 0.11	7.30 ± 0.55[a]	10.02 ± 0.37[a]	0	0	35
	GPi	Control	62.7 ± 2.8	0.20 ± 0.03	7.54 ± 0.23	10.65 ± 0.23	1.5	0	50
		GPe lesion	66.4 ± 4.6	0.18 ± 0.04	6.94 ± 0.28	10.00 ± 0.32	0	0	41
X	STN	Control	24.8 ± 2.6	0.97 ± 0.17	9.36 ± 0.42	12.35 ± 0.39	0	0	31
		GPe lesion	37.7 ± 2.9[a]	1.59 ± 0.29	7.78 ± 0.18[a]	11.04 ± 0.24	0	0	39
	GPi	Control	60.1 ± 5.6	0.33 ± 0.09	8.34 ± 0.59	11.16 ± 0.65	0	0	11
		GPe lesion	69.5 ± 3.5	0.35 ± 0.03	7.36 ± 0.15	10.89 ± 0.18	0	0	50

[a] $p < 0.05$ against individual control.

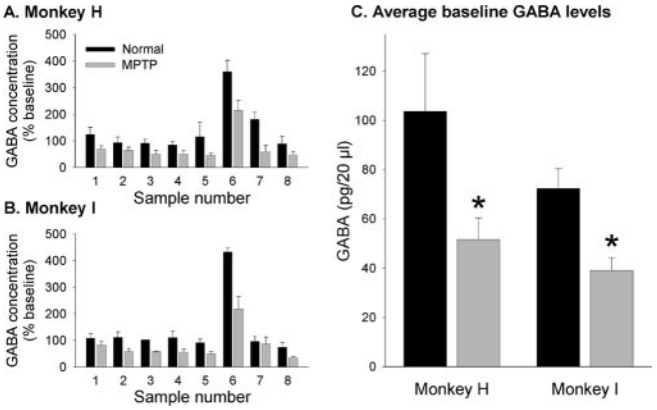

Figure 3. GABA concentrations in the STN as measured with microdialysis in monkeys H and I, before (black columns) and after (gray columns) treatment with MPTP. *A* and *B* show the average GABA levels by sample number in the two monkeys. Per our microdialysis protocol, sample 6 was exposed to 80 mM K^+, resulting in a significant increase in the GABA level. *C* depicts the average absolute baseline GABA levels in the two monkeys. *$p < 0.05$ versus the baseline level in the normal state.

kinsonian animals (Delfs et al., 1995; Herrero et al., 1996a) and are known to reduce phasic changes in discharge in GPe and GPi (Hamada and DeLong, 1992).

GPe activity changes and the development of parkinsonian motor signs

The current rate-based model of the pathophysiology of parkinsonism states that a reduction in GPe discharge leads to the development of the parkinsonian motor abnormalities via disinhibition of STN. This prediction is not supported by the results of our experiments. In contrast to the obvious MPTP-induced parkinsonism, large GPe lesions in normal animals, which, at least in two animals, involved substantial portions of the ventral pallidal motor territory, did not induce discernible motor signs of parkinsonism. These findings are similar to previous studies of smaller GPe lesions (Mink and Thach, 1991), which induced only a slight flexion bias and bradykinesia. As expected, the lesions in our monkeys induced changes in discharge rates in STN and GPi, which were comparable with those seen in the parkinsonian animals. However, GPe lesioned and MPTP-lesioned animals differed with regard to the induction of burst discharges and oscillatory discharge in the basal ganglia. Both parameters were greatly altered in the MPTP-treated animals but were not or only slightly affected in the GPe-lesioned monkeys.

Together, these studies suggest that a reduction in GPe activity and the resulting increases in STN and GPi activity may be necessary but are not sufficient to induce parkinsonism. The findings also suggest that changes in neuronal discharge patterns in the basal ganglia output nuclei may be as relevant as changes in discharge rate in the development of parkinsonian motor signs (Filion, 1979; Bergman et al., 1994; Hassani et al., 1996; Wichmann et al., 1999; Ni et al., 2000; Raz et al., 2000; Bevan et al., 2002; Wichmann and DeLong, 2003a). Even very early studies of the changes in neuronal discharge in the basal ganglia have remarked on the prominence of burst patterns and oscillatory discharge abnormalities in the basal ganglia of parkinsonian monkeys (Filion, 1979; Miller and DeLong, 1987; Filion and Tremblay, 1991; Bergman et al., 1994). Our results are in general agreement with results obtained in rodents in which pallidal lesions and dopamine depletion were also shown to differ (Hassani et al., 1996), although these recordings were performed in anesthetized animals, and behavioral comparisons between the experimental groups were not provided.

It is important to realize that the findings in the GPe-lesioned animals do not rule out the possibility that altered activity in GPe is involved in the development of parkinsonian motor abnormalities. Despite the fact that GPe ablation does not appear to result in the pattern abnormalities or motor abnormalities typical for parkinsonism, less drastic alterations of GPe activity may be relevant in this regard. For instance, it has been proposed that neurons participating in closed GPe-STN loops (Shink et al., 1996) may act as pacemakers (Plenz and Kitai, 1999), generating syn-

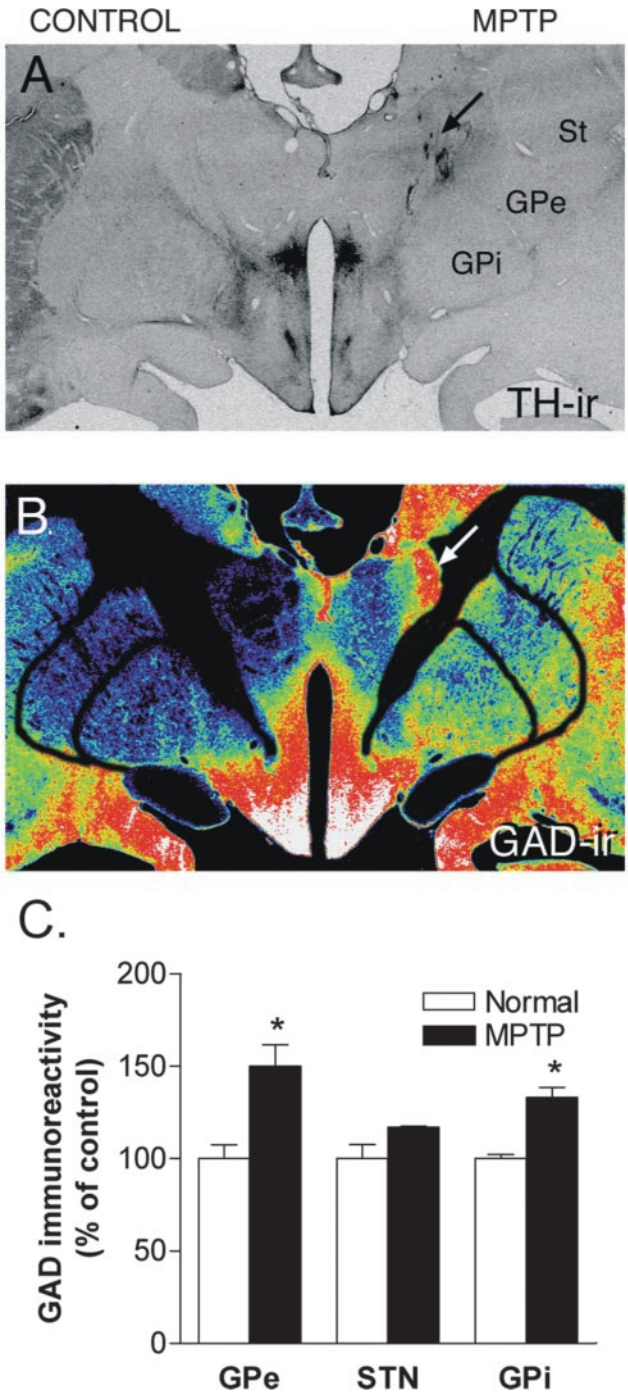

Figure 4. TH and GAD-IR in the basal ganglia. *A*, Macrograph showing TH-IR in the striatum (St) of monkey H. Note the presence and absence of TH-IR in the striatum in the control and lesioned sides, respectively. *B*, The same section was double labeled for GAD by immunoautoradiography. The gray levels have been converted to a pseudocolor scale, wherein red color depicts high immunoreactivity and blue depicts low immunoreactivity. Note the increase in GAD-IR in GPe and GPi on the lesioned side. The arrow indicates nonspecific staining along electrode and microdialysis tracts. *C*, Histograms depicting densitometric measurements of GAD-IR in GPe, STN, and GPi from the untreated (white columns) and MPTP-lesioned side (black columns). GAD-IR was quantified from immunoautoradiograms using the MCID image analysis system. GAD-IR is expressed as percentage control. ir, Immunoreactivity.

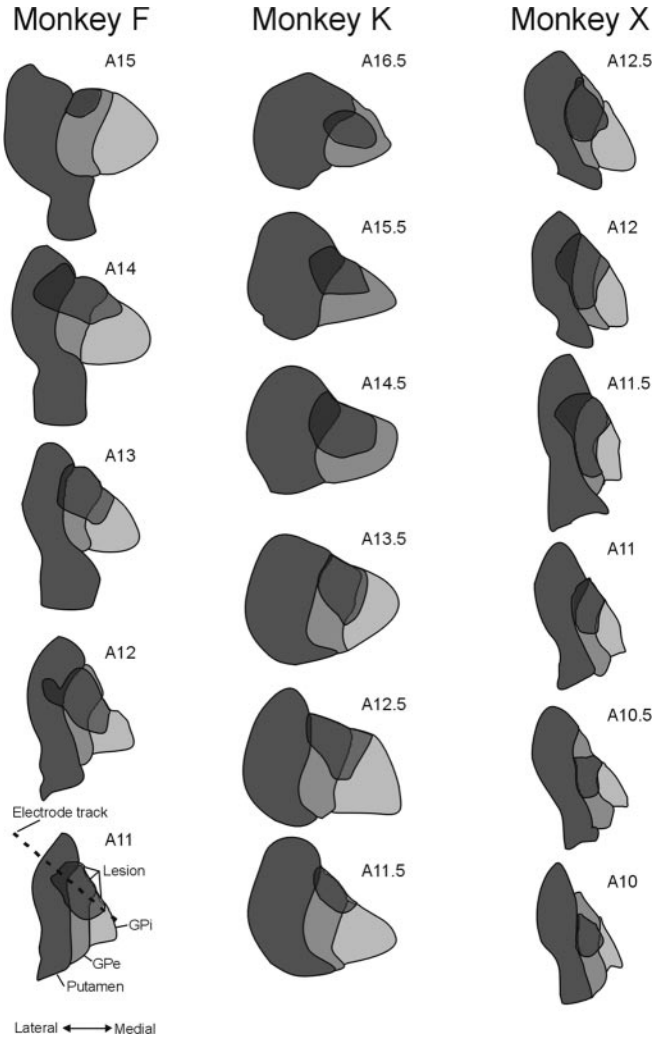

Figure 5. Extent of ibotenic acid-induced lesion aimed at GPe. Histological and electrophysiological data were used to reconstruct the location of the ibotenic acid injections in these serial coronal sections. The approximate anterior coronal plane number is shown in the top right corner of each diagram. As indicated in the diagram in the bottom left corner, the dark gray structures indicate the extent of the putamen, the medium gray structure indicates the extent of GPe, and the light gray structure indicates the extent of GPi. The lesions are shown as semitransparent overlays. The dashed line in the drawing in the bottom left corner shows the angle of approach to the pallidum, which was used for recording and lesioning penetrations.

chronized rhythmic bursts in both structures in dopamine-free coculture experiments. The occurrence and maintenance of such bursts may depend on, at least in part, the propensity of STN neurons to respond with rebound bursts to incoming synchronized volleys of activity along the GPe-STN pathway (Bevan et al., 2002). In favor of a role of GPe in the generation of oscillatory activity in STN and GPi is the fact that the proportion of cells engaged in oscillatory activity in GPe-lesioned animals appeared to be lower than in unlesioned animals (Fig. 2).

Alternatively, oscillatory and burst activity in STN and GPi may emerge independent of GPe input. For instance, it has been speculated that pattern abnormalities in STN may result from loss of dopamine in the STN (Meibach and Katzman, 1979; Campbell et al., 1985; Besson et al., 1988; Johnson et al., 1994; Kreiss et al., 1997; Francois et al., 2000; Smith and Kieval, 2000; Zhu et al., 2002) or from changes in the synchronization between STN neurons and cortex (Magill et al., 2000a,b, 2001; Wichmann et al., 2001b). Other explanations would include altered interactions between STN and brainstem areas such as the pedunculopontine nucleus (Orieux et al., 2000) or between STN and the intralaminar nuclei of the thalamus (Bacci et al., 2002).

Conclusions

Our experiments provide evidence that the neuronal activity in GPe is reduced in the parkinsonian state but do not support the concept that this reduction per se results in parkinsonism. The experiments emphasize the importance of changes in discharge patterns in the basal ganglia output nuclei for the development of parkinsonian motor signs. Although the importance of such changes is obvious, it remains to be seen whether network interactions between STN and GPe, cortex, brainstem or thalamus, or changes in the local milieu within STN are most relevant for the development of pattern changes. Perhaps even more importantly, it remains to be determined which pattern abnormalities are most deleterious for motor performance in parkinsonism.

References

Albin RL, Young AB, Penney JB (1989) The functional anatomy of basal ganglia disorders. Trends Neurosci 12:366–375.

Alexander GE, Crutcher MD (1990) Functional architecture of basal ganglia circuits: neural substrates of parallel processing. Trends Neurosci 13:266–271.

Alexander GE, Crutcher MD, DeLong MR (1990) Basal ganglia-thalamocortical circuits: parallel substrates for motor, oculomotor, "prefrontal" and "limbic" functions. Prog Brain Res 85:119–146.

Alvarez L, Macias R, Guridi J, Lopez G, Alvarez E, Maragoto C, Teijeiro J, Torres A, Pavon N, Rodriguez-Oroz MC, Ochoa L, Hetherington H, Juncos J, DeLong MR, Obeso JA (2001) Dorsal subthalamotomy for Parkinson's disease. Mov Disord 16:72–78.

Bacci JJ, Kerkerian-Le Goff L, Salin P (2002) Effects of intralaminar thalamic nuclei lesion on glutamic acid decarboxylase (GAD65 and GAD67) and cytochrome oxidase subunit I mRNA expression in the basal ganglia of the rat. Eur J Neurosci 15:1918–1928.

Bankiewicz KS, Oldfield EH, Chiueh CC, Doppman JL, Jacobowitz DM, Kopin IJ (1986) Hemiparkinsonism in monkeys after unilateral internal carotid artery infusion of 1-methyl-4-phenyl-1,2,3,6-tetrahydropyridine (MPTP). Life Sci 39:7–16.

Baron MS, Wichmann T, Ma D, DeLong MR (2002) Effects of transient focal inactivation of the basal ganglia in parkinsonian primates. J Neurosci 22:592–599.

Bergman H, Wichmann T, DeLong MR (1990) Reversal of experimental parkinsonism by lesions of the subthalamic nucleus. Science 249:1436–1438.

Bergman H, Wichmann T, Karmon B, DeLong MR (1994) The primate subthalamic nucleus. II. Neuronal activity in the MPTP model of parkinsonism. J Neurophysiol 72:507–520.

Besson MJ, Graybiel AM, Nastuk MA (1988) [3H]SCH 23390 binding to D1 dopamine receptors in the basal ganglia of the cat and primate: delineation of striosomal compartments and pallidal and nigral subdivisions. Neuroscience 26:101–119.

Bevan MD, Magill PJ, Terman D, Bolam JP, Wilson CJ (2002) Move to the rhythm: oscillations in the subthalamic nucleus-external globus pallidus network. Trends Neurosci 25:525–531.

Campbell GA, Eckardt MJ, Weight FF (1985) Dopaminergic mechanisms in subthalamic nucleus of rat: analysis using horseradish peroxidase and microiontophoresis. Brain Res 333:261–270.

Delfs JM, Ciaramitaro VM, Parry TJ, Chesselet MF (1995) Subthalamic nucleus lesions: widespread effects on changes in gene expression induced by nigrostriatal dopamine depletion in rats. J Neurosci 15:6562–6575.

DeLong MR (1990) Primate models of movement disorders of basal ganglia origin. Trends Neurosci 13:281–285.

Donzanti BA, Yamamoto BK (1988) A rapid and simple HPLC microassay for biogenic amines in discrete brain regions. Pharmacol Biochem Behav 30:795–799.

Filion M (1979) Effects of interruption of the nigrostriatal pathway and of dopaminergic agents on the spontaneous activity of globus pallidus neurons in the awake monkey. Brain Res 178:425–441.

Filion M, Tremblay L (1991) Abnormal spontaneous activity of globus pallidus neurons in monkeys with MPTP-induced parkinsonism. Brain Res 547:142–151.

Francois C, Savy C, Jan C, Tande D, Hirsch EC, Yelnik J (2000) Dopaminergic innervation of the subthalamic nucleus in the normal state, in MPTP-treated monkeys, and in Parkinson's disease patients. J Comp Neurol 425:121–129.

Gill SS, Heywood P (1997) Bilateral dorsolateral subthalamotomy for advanced Parkinson's disease. Lancet 350:1224.

Guridi J, Luquin MR, Guillen J, Herrero MT, Obeso JA (1993) Antiparkinsonian effect of subthalamotomy in MPTP-monkeys of different severity. Mov Disord 9:1910.

Hamada I, DeLong MR (1992) Excitotoxic acid lesions of the primate subthalamic nucleus result in reduced pallidal neuronal activity during active holding. J Neurophysiol 68:1859–1866.

Hassani OK, Mouroux M, Feger J (1996) Increased subthalamic neuronal activity after nigral dopaminergic lesion independent of disinhibition via the globus pallidus. Neuroscience 72:105–115.

Herrero MT, Ruberg M, Hirsch EC, Guridi J, Luquin MR, Guillen J, Javoy-Agid F, Agid Y, Obeso JA (1993) Changes in GAD mRNA expression in neurons of the internal pallidum in parkinsonian monkeys after L-DOPA therapy. Soc Neurosci Abstr 19:132.

Herrero MT, Levy R, Ruberg M, Javoy-Agid F, Luquin MR, Agid Y, Hirsch EC, Obeso JA (1996a) Glutamic acid decarboxylase mRNA expression in medial and lateral pallidal neurons in the MPTP-treated monkeys and patients with Parkinson's disease. Adv Neurol 69:209–216.

Herrero MT, Levy R, Ruberg M, Luquin MR, Villares J, Guillen J, Faucheux B, Javoy-Agid F, Guridi J, Agid Y, Obeso JA, Hirsch EC (1996b) Consequence of nigrostriatal denervation and L-dopa therapy on the expression of glutamic acid decarboxylase messenger RNA in the pallidum. Neurology 47:219–224.

Johnson AE, Coirini H, Kallstrom L, Wiesel FA (1994) Characterization of dopamine receptor binding sites in the subthalamic nucleus. NeuroReport 5:1836–1838.

Kreiss DS, Mastropietro CW, Rawji SS, Walters JR (1997) The response of subthalamic nucleus neurons to dopamine receptor stimulation in a rodent model of Parkinson's disease. J Neurosci 17:6807–6819.

Legendy CR, Salcman M (1985) Bursts and recurrences of bursts in the spike trains of spontaneously active striate cortex neurons. J Neurophysiol 53:926–939.

Magill PJ, Bolam JP, Bevan MD (2000a) Relationship of activity in the subthalamic nucleus-globus pallidus network to cortical electroencephalogram. J Neurosci 20:820–833.

Magill PJ, Bolam JP, Bevan MD (2000b) Neuronal activity in the globus pallidus during cortical inactivation in normal and 6-OHDA treated rats *in vivo*. Soc Neurosci Abstr 26:961.

Magill PJ, Bolam JP, Bevan MD (2001) Dopamine regulates the impact of the cerebral cortex on the subthalamic nucleus-globus pallidus network. Neuroscience 106:313–330.

Meibach RC, Katzman R (1979) Catecholaminergic innervation of the subthalamic nucleus: evidence for a rostral condition of the A9 (substantia nigra) dopaminergic cell group. Brain Res 173:364–368.

Miller WC, DeLong MR (1987) Altered tonic activity of neurons in the globus pallidus and subthalamic nucleus in the primate MPTP model of parkinsonism. In: The basal ganglia II (Carpenter MB, Jayaraman A, eds), pp 415–427. New York: Plenum.

Mink JW, Thach WT (1991) Basal ganglia motor control. III. Pallidal ablation: normal reaction time, muscle cocontraction, and slow movement. J Neurophysiol 65:330–351.

Ni Z, Bouali-Benazzouz R, Gao D, Benabid AL, Benazzouz A (2000) Changes in the firing pattern of globus pallidus neurons after the degeneration of nigrostriatal pathway are mediated by the subthalamic nucleus in the rat. Eur J Neurosci 12:4338–4344.

Olson RJ, Justice Jr JB (1993) Quantitative microdialysis under transient conditions. Anal Chem 65:1017–1022.

Orieux G, Francois C, Feger J, Yelnik J, Vila M, Ruberg M, Agid Y, Hirsch EC (2000) Metabolic activity of excitatory parafascicular and pedunculopontine inputs to the subthalamic nucleus in a rat model of Parkinson's disease. Neuroscience 97:79–88.

Pedneault S, Soghomonian JJ (1994) Glutamate decarboxylase (GAD65) mRNA levels in the striatum and pallidum of MPTP-treated monkeys. Brain Res Mol Brain Res 25:351–354.

Plenz D, Kitai S (1999) A basal ganglia pacemaker formed by the subthalamic nucleus and external globus pallidus. Nature 400:677–682.

Raz A, Vaadia E, Bergman H (2000) Firing patterns and correlations of spontaneous discharge of pallidal neurons in the normal and the tremulous 1-methyl-4-phenyl-1,2,3,6-tetrahydropyridine vervet model of parkinsonism. J Neurosci 20:8559–8571.

Robertson RG, Graham WC, Sambrook MA, Crossman AR (1991) Further investigations into the pathophysiology of MPTP-induced parkinsonism in the primate: an intracerebral microdialysis study of gamma-aminobutyric acid in the lateral segment of the globus pallidus. Brain Res 563:278–280.

Salin P, Manrique C, Forni C, Kerkerian-Le Goff L (2002) High-frequency stimulation of the subthalamic nucleus selectively reverses dopamine denervation-induced cellular defects in the output structures of the basal ganglia in the rat. J Neurosci 22:5137–5148.

Schneider JS, Wade TV (2003) Experimental parkinsonism is associated with increased pallidal GAD gene expression and is reversed by site-directed antisense gene therapy. Mov Disord 18:32–40.

Schroeder JA, Schneider JS (2001) Alterations in expression of messenger RNAs encoding two isoforms of glutamic acid decarboxylase in the globus pallidus and entopeduncular nucleus in animals symptomatic for and recovered from experimental Parkinsonism. Brain Res 888:180–183.

Sellal F, Hirsch E, Lisovoski F, Mutschler V, Collard M, Marescaux C (1992) Contralateral disappearance of parkinsonian signs after subthalamic hematoma. Neurology 42:255–256.

Shink E, Bevan MD, Bolam JP, Smith Y (1996) The subthalamic nucleus and the external pallidum: two tightly interconnected structures that control the output of the basal ganglia in the monkey. Neuroscience 73:335–357.

Smith Y, Kieval JZ (2000) Anatomy of the dopamine system in the basal ganglia. Trends Neurosci 23:S28–S33.

Soghomonian JJ, Chesselet MF (1992) Effects of nigrostriatal lesions on the levels of messenger RNAs encoding two isoforms of glutamate decarboxylase in the globus pallidus and entopeduncular nucleus of the rat. Synapse 11:124–133.

Soghomonian JJ, Laprade N (1997) Glutamate decarboxylase (GAD67 and GAD65) gene expression is increased in a subpopulation of neurons in the putamen of Parkinsonian monkeys. Synapse 27:122–132.

Soghomonian JJ, Pedneault S, Audet G, Parent A (1994) Increased glutamate decarboxylase mRNA levels in the striatum and pallidum of MPTP-treated primates. J Neurosci 14:6256–6265.

Vila M, Levy R, Herrero MT, Ruberg M, Faucheux B, Obeso JA, Agid Y, Hirsch EC (1997) Consequences of nigrostriatal denervation on the functioning of the basal ganglia in human and nonhuman primates: an *in situ* hybridization study of cytochrome oxidase subunit I mRNA. J Neurosci 17:765–773.

Wichmann T, DeLong MR (2003a) Pathophysiology of Parkinson's disease: the MPTP primate model of the human disorder. Ann NY Acad Sci 991:199–213.

Wichmann T, DeLong MR (2003b) Functional neuroanatomy of the basal ganglia in Parkinson's disease. Adv Neurol 91:9–18.

Wichmann T, Bergman H, Starr PA, Subramanian T, Watts RL, DeLong MR (1999) Comparison of MPTP-induced changes in spontaneous neuronal discharge in the internal pallidal segment and in the substantia nigra pars reticulata in primates. Exp Brain Res 125:397–409.

Wichmann T, Kliem MA, DeLong MR (2001a) Antiparkinsonian and behavioral effects of inactivation of the substantia nigra pars reticulata in hemiparkinsonian primates. Exp Neurol 167:410–424.

Wichmann T, Kliem MA, Soares J (2001b) Correlation between neuronal discharge in the basal ganglia and EEG in normal and parkinsonian primates. Soc Neurosci Abstr 27:749.23.

Winters WD, Kado RT, Adey WR (1969) A stereotaxic brain atlas for *Macaca nemestrina*. Berkeley, CA: Berkeley California Press.

Zhu Z, Bartol M, Shen K, Johnson SW (2002) Excitatory effects of dopamine on subthalamic nucleus neurons: *in vitro* study of rats pretreated with 6-hydroxydopamine and levodopa. Brain Res 945:31–40.